

8504

College of Engineering  
Virginia Polytechnic Institute & State University  
Blacksburg, Virginia 24061

VPI-E-74-29

EFFECTS OF ARTIFICIAL CRACKS  
AND POISSON'S RATIO UPON PHOTOELASTIC  
STRESS INTENSITY DETERMINATION

M. Jolles\*, J. J. McGowan\*\* and C. W. Smith\*\*\*

Department of Engineering Science & Mechanics

November 1974 RETURN TO: AFOSPACE STRUCTURES  
INFORMATION AND ANALYSIS CENTER

AFDL/FBR  
WPAFB, OHIO 45433

Reporting Period: Spring 1974 through Fall 1974

Prepared For:

National Science Foundation  
Grant No. GK 39922  
Washington, D. C.

Approved for Public Release; distribution unlimited.

20000111 086

\*Lecturer

\*\*Assistant Professor

\*\*\*Professor

Department of Engineering Science & Mechanics  
Virginia Polytechnic Institute & State University  
Blacksburg, Virginia 24061

Reproduced From  
Best Available Copy

- |  |   |  |
|--|---|--|
| 1. Report No.<br>VPI-E-74-29   | 2. Government Accession No.<br>_____  | 3. Recipients Cat. No.<br>_____                            |
| 4. Title<br>EFFECTS OF ARTIFICIAL CRACKS AND POISSON'S RATIO<br>UPON PHOTOELASTIC STRESS INTENSITY DETERMINATION   | 5. Report Date<br>October 1974  | 8. Performing Organization<br>Report Number<br>VPI-E-74-29 |
| 7. Authors<br>M. Jolles, J. J. McGowan and C. W. Smith   | 10. Work Unit No.   | 11. Contract or Grant No.<br>GK 39922                      |
| 9. Performing Organization Name & Address<br>Department of Engineering Science & Mechanics<br>Virginia Polytechnic Institute & State University<br>Blacksburg, Virginia 24061  | 13. Type of Report &<br>Period Covered<br>Summer & Fall 1974                              |  |
| 12. Sponsoring Agency Name and Address<br>National Science Foundation<br>Washington, D. C.   |   |  |
| 16. Abstract<br><p>A series of stress freezing photoelastic experiments were performed with multiple replications upon edge cracked strips for three types of "cracks" in current use: i) Rectangular slots 0.152 mm wide, ii) 1.59 mm wide slots terminating in a 30° vee notch of approximately 0.025 mm root radius, and iii) Natural cracks (approximately 0.0025 mm root radius). Stress intensity results were compared with the Gross-Srawley Analysis; in addition (i) was compared with Savin's solution. It was concluded that (ii) and (iii) yield the same results but (i) was slightly higher. Both (ii) and (iii) were about 12% higher than the Gross-Srawley results. This is conjectured to be related to a Poisson's Ratio Effect.</p> |   |  |
| 17. Key Words<br>Stress Intensity Factors,<br>Fracture Mechanics, Photoelasticity,<br>Edge Cracks, Stress Freezing   | 18. Distribution Statement<br>Approved for public re-<br>lease; distribution<br>unlimited |  |
| 19. Security Classif. (report)<br>Unclassified   | 20. Security Classif. (page)<br>Unclassified  |  |

# LIST OF SYMBOLS

$r, \theta$	Polar coordinates as defined in Figure 1 (mm, rad)
$x, y$	Cartesian coordinates as defined in Figure 1 (mm)
$\sigma_{ij}$	Stress Components $i, j = 1, 2$ (KPa)
$\epsilon_{ij}$	Strain Components $i, j = 1, 2$ (mm/mm)
$u_i$	Displacement Components $i = 1, 2$ (mm)
$\tau_{\max}$	Maximum in plane shearing stress (KPa)
$K_I$	Mode I Stress Intensity Factor (KPa-m <sup>1/2</sup> )
$K_{AP}$	Apparent Mode I Stress Intensity Factor (KPa-m <sup>1/2</sup> )
	$K_{AP} = \tau_{\max}(8\pi r)^{1/2}$
$K_{TSCM}$	Estimated $K_I$ by TSCM (KPa-m <sup>1/2</sup> )
$s$	Length along curved path (mm)
$g_I$	Mode I strain energy release rate (J/m <sup>2</sup> )
$E$	Modulus of Elasticity (GPa)
$\nu$	Poisson's Ratio

## TABLE OF CONTENTS

Introduction . . . . .	1
Analytical Considerations . . . . .	2
i) TSCM . . . . .	3
ii) Poisson's Ratio Effect . . . . .	4
The Experiments . . . . .	6
Results and Discussion . . . . .	7
Summary and Conclusions . . . . .	9
Acknowledgements . . . . .	9
References . . . . .	10

## TABLES

I - Test Results for Edge Cracks . . . . .	13
--	----

## FIGURES

1 Notation . . . . .	14
2 Spreading of Fringes Normal to Crack Plane (Mode I) . . . . .	15
3 Generalized Plate Specimen . . . . .	16
4 Specimen Geometry and Loading . . . . .	17
5 Normalized $K_{Ap}$ vs $r^{1/2}$ A Typical Result . . . . .	18
6 Normalized $K_{Ap}$ vs $r^{1/2}$ Rectangular Slot . . . . .	19

## Introduction

The idea of obtaining stress intensity factors (SIF) from photoelastic results was suggested by G. R. Irwin [1] in the early 1950's. Since that time, a number of investigators have contributed to efforts to obtain SIF values from photoelastic data. The early work of Post and Wells and Post [2], [3] studies by Fessler and Mansell [4], by Marloff et al [5], by Liebowitz, Vanderveldt, and Sanford [6], by Kobayashi and his associates [7], [8], [9] and recently by the senior author and his associates [10]-[25] has led to both a clarification and means for overcoming difficulties associated with application of the method. The most important current difficulties appear to be:

- i) Accuracy with which the SIF may be extracted from photoelastic data.
- ii) A means for constructing "artificial" cracks of known geometry and their susceptibility to finite deformation effects in stress freezing.
- iii) The influence upon local constraint of the high Poisson's Ratio ( $\nu \approx 0.5$ ) encountered in stress freezing work.

Over a period of five years, the senior author and his associates have evolved a technique for extracting the stress intensity factor directly from photoelastic data, without resorting to stress separation methods. This approach met with success in dealing with three dimensional Mode I problems. The technique employs a representation of the maximum in-plane shearing stress as a singular term plus a Taylor series to account for effects of the regular stress field in the data zone. Referred to as a Taylor Series Correction Method (TSCM), it is described elsewhere [16], [17], [19], [20] and is believed to be useful in overcoming the difficulty noted in Item i).

An extensive photoelastic investigation of crack-like notches was conducted by Dixon and Strannigan [26] some years ago. However, the thrust

of this work was not directed towards direct SIF determination. Recently, Gross and Mendelson [27] found analytically that vee notches of  $30^\circ$  or less would simulate notch tip stress fields which lead to agreement to within 2% of SIF values for natural cracks. This led the senior author to examine various vee notch angles photoelastically for compact tension specimens [18]. His results confirmed the findings of Gross and Mendelson but the confirmation was done primarily at room temperature.

The writers have had occasion to employ "artificial" cracks in several instances in order to achieve uniform and repeatable crack geometries. In so doing, they have found two types of notches convenient to use:

a) A 0.152 mm wide rectangular tipped slot

b) 1.59 mm wide slots terminating in a vee notch of approximately 0.025 mm root radius. A primary goal of this study is to assess how well these notches simulate natural cracks in stress freezing work.

When one conducts stress freezing experiments, care must be taken to avoid gross field finite deformations. Moreover, for a cracked plate of finite thickness, a state of nearly plane strain exists near the crack tip. However, remote from the crack tip the states of stress and deformation are well characterized by generalized plane stress. Since a zone of transition must lie between these extremes, the problem becomes three dimensional and thus dependent upon Poisson's Ratio. Since all stress freezing materials exhibit a value of Poisson's Ratio of  $\approx 0.5$ , and since  $\nu \approx 0.3$  for most structural materials, the influence of the "artificially" elevated value of Poisson's Ratio needs to be examined. A secondary goal of this paper is to examine this effect.

#### Analytical Considerations

Although these topics are treated elsewhere in the open literature, a brief discussion of concepts applied to the present study is included here

for convenience.

The TSCM [16][17][19][20] - As is well known, the elastic stress field surrounding the crack tip can be expressed, for the Mode I case as:

$$\sigma_{ij} = \frac{K_I}{(2\pi r)^{1/2}} f_{ij}(\theta) \quad \dots i, j = x, y \dots \quad (1)$$

with the notation given in Figure 1. By substituting Equation 1 into Equation 2

$$\tau_{\max} = 1/2 \left[ (\sigma_x - \sigma_y)^2 + 4\tau_{xy}^2 \right]^{1/2} \quad (2)$$

one obtains

$$\tau_{\max} = f(r, \theta, K_I) \quad (3)$$

and since, for Mode I loadings, the fringe loops tend to spread in a direction approximately normal to the crack surfaces (Figure 2), we may evaluate  $\tau_{\max}$  along  $\theta = \pi/2$ , yielding

$$\tau_{\max} = \frac{K_I}{(8\pi r)^{1/2}} \quad (4)$$

Moreover, since the stress-optic law prescribes

$$\tau_{\max} = \frac{nf}{2t} \quad (5)$$

a relationship of the fringe order to  $K_I$  is established. In obtaining data along  $\theta = \pi/2$  some of the points may be far enough away from the crack tip to be influenced by the regular stress field. In order account for this, we use a Taylor series to represent the regular part of the stress field. Thus,

$$\tau_{\max} = \frac{K_I}{(8\pi r)^{1/2}} + \sum_{N=0}^M B_N r^{N/2} \quad (6)$$

becomes the equation to which values of  $K_I$  are fitted by a least squares process in TSCM. This result corresponds to the Williams Stress Function

for two dimensional problems and reduces to the Irwin two parameter method. to within truncation error for a three term expression for  $\tau_{\max}$ .

#### Poisson's Ratio Effect [28][29][30]

The experimentally determined SIF for a plate containing a through crack is known [28][29] to yield a higher result than the corresponding two dimensional solution. This difference in SIF values is due to the fact that a constraint develops near the crack tip in the experiment since the plate thickness is much greater than the crack root radius and a state of nearly plane strain results local to the crack tip. At distances which are substantially larger than the thickness from the crack tip, a state of nearly generalized plane stress will result. As noted earlier, a zone of transition will exist between these extremes, resulting in a three dimensional problem. Brown and Srawley [29], and Irwin [30], have pointed out that the two dimensional result can be converted to the three dimensional SIF by multiplying the SIF by  $(1 - \nu^2)^{-1/2}$ . A rationale for this conversion can be constructed as follows:

Consider the Mode I traction loaded cracked plate of Figure 3. Rice [31] has identified an integral:

$$J = \int [U dy - \sigma_i \frac{\partial u_i}{\partial x} ds] \quad (7)$$

where  $U = \frac{1}{2} \sigma_{ij} \epsilon_{ij}$ , the strain energy density,

$u_i$  = displacement components

$\sigma_i$  = stress vector components

which is independent of path for two dimensional problems. Moreover, if the strain energy density is a quadratic function of the strains, the J integral is identical to the strain energy release rate g.



If we compute  $J_I$  for Path A, which is located at distances substantially larger than the plate thickness from the crack tip, the result will be approximately the strain energy release rate for plane stress as computed by Paris and Sih [32]. Thus

$$J_I = g_I \approx \frac{K_{IA}^2}{E} \quad (8)$$

On the other hand, locating the path B within the constrained region, we would expect our result to be approximately the plane strain  $g$  value, or

$$J_I = g_I = \frac{(1 - \nu^2)K_{IB}^2}{E} \quad (9)$$

For  $J_I$  to be path independent, it follows that  $K_{IB} = (1 - \nu^2)^{-1/2} K_{IA}$ .

In real plate problems the thickness is finite, and the preceding conversion becomes a maximum conversion factor. If the thickness is large relative to the lateral dimensions of the body, no conversion would be required. It is only where the thickness is substantially less than the lateral dimensions of the body that the two dimensional solution will agree with the plane stress result.

Alternatively, if we multiply the SIF measured photoelastically at the crack tip by  $(1 - \nu)^{1/2}$ , we get the SIF which corresponds to the two dimensional solution for a thin plate. In stress freezing work,  $\nu = 0.5$  and if we wish to obtain the test result which would correspond to Poisson's ratio  $\approx 0.3$ , we can convert the two dimensional result back to the test result form using the inverse of the above conversion. Our complete conversion factor is then:

$$\frac{[1 - (0.5)^2]^{1/2}}{[1 - (0.3)^2]^{1/2}} = 0.91$$

for correcting the "plane strain" test result for the fact that Poisson's Ratio was different for the test material than for the prototype structural material. This effect is further verified in [33].

## The Experiments

A series of stress freezing photoelastic experiments were designed using an edge cracked strip as the test model. This model was selected because, due to bending effects and lack of gross constraint, it was very sensitive to small load changes and also because accurate analytical solutions such as that of reference [34] were available. The basic specimen geometry and loading is pictured in Figure 4 together with the three types of cracks studied. Beginning with stress free strips of PSM-8 (Photolastic, Inc.) natural cracks were tapped into the plate edge, while the "artificial" cracks were inserted with circular saws. Specimens were then placed in the stress freezing oven in a string loaded tensile load rig as indicated in Figure 4. After heating to critical temperature and soaking to achieve uniform temperature, loads were applied and the specimens were cooled under load. Two load levels were employed. One load level corresponded essentially to about 80% of the threshold value for slow crack growth of the natural crack, and, twice this load was also used for the artificial cracks. For natural cracks, half of this load or 40% of the threshold value was also employed. A summary of the tests run together with average data values are found in the upper part of Table I.

The frozen slices were then coated with an oil of the same index of refraction as the model material and inserted into the field of Photolastic Model 051 Slice Analyzer for fringe order determination along a line normal to the crack surfaces and passing through the crack tip.

In addition to the stress freezing tests, tests were conducted on Vee-notched and naturally cracked specimens at room temperature at which the material's Poisson's Ratio was 0.36.

## Results and Discussion

A set of test data from one of the V-H tests (Table I) are plotted in Figure 5 which may be regarded as typical for all tests. This plot of normalized apparent SIF,  $K_{Ap}/\sigma(\pi a)^{1/2}$  vs  $(r/a)^{1/2}$  is used to interpret the data and to extrapolate the portion of the data in the appropriate zone to obtain the SIF. In his discussion [1] Irwin pointed out that at least two parameters were necessary to obtain the SIF in a two dimensional problem. This leads to an equation for  $\tau_{max}$  which corresponds to Equation 6 with  $M = 0$ . Moreover, it implies that a plot of the data such as given by Figure 5 should yield a straight line in the zone dominated by the singular stresses. Thus, in the present study,  $M$  was set equal to zero in the computer program and only the data in Zone II of Figure 5 were used in obtaining  $K_{TSCM}$ .

In Zone I, effects of the regular stress field are significant; and in Zone III, recent studies [25] indicate that the stress relaxation here is due to material non-linearity near the crack or notch tip. Zone II occurred in the same  $r/a$  range for all crack geometries.

From a study of the average values of  $\left[ \frac{K_{TSCM}}{K_{Th}} \right]$  in Table I, it is concluded that all experimental results were higher than predicted by the two dimensional theory with the rectangular cracks exhibiting SIF values of over 20% above analytical results. The vee notches and the natural cracks yielded essentially the same results which averaged 12% above the two dimensional solution. Since the SIF reproducibility of the "artificial" cracks was to within  $\pm 2.5\%$  and for the natural cracks  $\pm 4\%$ , the above results clearly represent a definite data trend.

Upon applying the conversion factor of 0.91 noted earlier to the test results, the natural and vee-notch cracks agree with the two dimensional solution to within  $\pm 3\%$  for the stress freezing tests and within 1% for the room temperature tests. The rectangular slots, however, still average 10% above the two dimensional solution.

The rectangular slot was studied by Schroedl and Smith [24]. Using their computer program for Savin's solution, the authors constructed Figure 6. From this graph it is clear that, if data in the  $(r/a)^{1/2}$  range of 0.2 to 0.4 are linearly extrapolated to the origin for the rectangular slot,  $(b/a = 0.006)$  a normalized SIF results which is about 6% greater than for the line crack. The balance of the difference (Table I) is attributed to finite deformation effects at the higher load.

By comparing Figures 5 and 6, it is clear that the singularity introduced by the presence of the square corner in Figure 6 is absent from Figure 5. This is believed to be due to the fact that material nonlinearities develop in the zone of high  $K_{AP}/K_{Th}$  values. However, in any case, one can still obtain valid values of the SIF with rectangular slots at lower loads by taking data outside of  $(r/a)^{1/2} \approx 0.3$  to 0.4 provided the data are linear there.

The rather significant Poisson's Ratio effect noted here in stress freezing work on two dimensional problems naturally raises the question as to the extent of this effect in three dimensional problems where generalized plane stress does not exist away from the crack tip. By studying existing approximate solutions to such problems such as [35] one can conjecture that the effect will generally be less than the usual experimental error of 5%. More exact information, however, will require further study.

It is noted that only one plate thickness was studied here and the authors hope to extend their results to other thicknesses in future work.

## Summary and Conclusions

A stress freezing photoelastic study was carried out on a series of edge cracked strips containing three types of cracks. It was concluded that:

- i) 1.59 mm wide slots terminating in a 30° vee notch of approximately 0.025 mm root radius yield essentially the same SIF values as natural cracks.
- ii) Test results can be replicated to within  $\pm 4\%$ .
- iii) The effect of Poisson's Ratio in a stress freezing plate test is significant and should be accounted for when comparing results with two dimensional solutions. An approximate means for doing this is described.
- iv) Rectangular slots 0.152 mm wide tend to give SIF values which are some 10 percent higher than vee notch or natural crack results. This effect can be alleviated by utilizing data further from the crack tip provided the data are still linear in Fig. 5 and by keeping loads quite small.

The present studies were quite restrictive in terms of both test and crack geometries. However, it is hoped that useful quantitative information on photoelastic stress intensity determination has resulted. Studies directed to improve the accuracy of the method are continuing.

## Acknowledgements

The authors wish to acknowledge the contributions of B. E. Gross, J. E. Srawley, W. F. Brown, A. Mendelson, and G. R. Irwin upon whose works they have drawn for these studies. The authors also appreciate the interest and support of D. Frederick and C. J. Astill. This study was supported by the National Science Foundation under Grant No. GK 39922.

### References

- [1] Irwin, G. R., Discussion, Proceedings of the Society for Experimental Stress Analysis 16, 1, 92-96 (1958).
- [2] Post, D., "Photoelastic Stress Analysis for an Edge Crack in a Tensile Field", Proceedings of the Society for Experimental Stress Analysis 12, 1, 99-116 (1954).
- [3] Wells, A. A. and Post, D., "The Dynamic Stress Distribution Surrounding a Running Crack - A Photoelastic Analysis", Proceedings of the Society for Experimental Stress Analysis 16, 1, 69-92 (1958).
- [4] Fessler, H. and Mansell, D. O., "Photoelastic Study of Stresses Near Cracks in Thick Plates", Journal of Mechanical Engineering Science 4, 3, 213-225 (1962).
- [5] Marloff, R. H., Levin, M. M., Johnson, R. L., and Ringler, T. N., "Photoelastic Determination of Stress Intensity Factors", Experimental Mechanics 11, 12, 529-539, December 1971.
- [6] Liebowitz, H., Vanderveldt, H. and Sanford, R. J., "Stress Concentrations Due to Sharp Notches", Experimental Mechanics 7, 12, 513-517, December 1967.
- [7] Bradley, W. B. and Kobayashi, A. S., "An Investigation of Propagating Cracks by Dynamic Photoelasticity", Experimental Mechanics 10, 3, 106-113, March 1970.
- [8] Bradley, W. B. and Kobayashi, A. S., "Fracture Dynamics - A Photoelastic Investigation", J. of Engineering Fracture Mechanics 3, 3, 317-332, October 1971.
- [9] Kobayashi, A. S. and Wade, B. G., "Crack Propagation and Arrest in Impacted Plates", TR-13 Dept. of Mechanical Engineering, College of Engineering, University of Washington, Seattle, Wash., June 1972.
- [10] Smith, D. G. and Smith, C. W., "A Photoelastic Evaluation of the Influence of Closure and Other Effects Upon the Local Bending Stresses in Cracked Plates", International Journal of Fracture Mechanics 6, 3, 305-318, September 1970.
- [11] Smith, D. G. and Smith, C. W., "Influence of Precatastrophic Extension and Other Effects on Local Stresses in Cracked Plates Under Bending Fields", Experimental Mechanics 11, 9, 394-401, September 1971.
- [12] Smith, D. G. and Smith, C. W., "Photoelastic Determination of Mixed Mode Stress Intensity Factors", J. of Engineering Fracture Mechanics 4, 2, 357-366, June 1972.
- [13] Marrs, G. R. and Smith, C. W., "A Study of Local Stresses Near Surface Flaws in Bending Fields", Stress Analysis and Growth of Cracks, ASTM STP 513, 22-36 (October 1972).

- [14] Schroedl, M. A., McGowan, J. J. and Smith, C. W., "An Assessment of Factors Influencing Data Obtained by the Photoelastic Stress Freezing Technique for Stress Fields Near Crack Tips", J. of Engineering Fracture Mechanics 4, 4, 801-809, December 1972.
- [15] Schroedl, M. A. and Smith, C. W., "Local Stresses Near Deep Surface Flaws Under Cylindrical Bending Fields", Progress in Flaw Growth and Fracture Toughness Testing ASTM STP 536, 45-63, October 1973.
- [16] Schroedl, M. A., McGowan, J. J. and Smith, C. W., "Determination of Stress Intensity Factors from Photoelastic Data with Application to Surface Flaw Problems", Experimental Mechanics 14, 10, 392-399, October 1974.
- [17] Harms, A. E. and Smith, C. W., "Stress Intensity Factors in Long, Deep Surface Flaws in Plates Under Extensional Fields", VPI-E-73-6, 37 pages, February 1973 (In Press) Proceedings of the Tenth Anniversary of the Society for Engineering Science.
- [18] Schroedl, M. A. and Smith, C. W., "Influence of Three Dimensional Effects on the Stress Intensity Factor for Compact Tension Specimens", Fracture Analysis ASTM STP 560, 69-80, October 1974.
- [19] Smith, C. W., "Use of Three Dimensional Photoelasticity in Fracture Mechanics" (Invited Paper) Experimental Mechanics 13, 12, 539-544, December 1973. Also (In Press) Proceedings of the Third International Congress on Experimental Mechanics.
- [20] Schroedl, M. A., McGowan, J. J. and Smith, C. W., "Use of a Taylor Series Correction Method in Photoelastic Stress Intensity Determinations", VPI-E-73-34, 31 pages, November 1973 Spring Meeting SESA, Detroit, Mich., May 1974.
- [21] Mullinix, B. R. and Smith, C. W., "Distribution of Local Stresses Across the Thickness of Cracked Plates Under Bending Fields", International Journal of Fracture 10, 3, 337-352, September 1974.
- [22] McGowan, J. J. and Smith, C. W., "Stress Intensity Factors for Deep Cracks Emanating from the Corner Formed by a Hole Intersecting a Plate Surface", VPI-E-74-1, 23 pages, January 1974, Eighth National Symposium on Fracture Mechanics, Brown University, August 1974.
- [23] Jolles, M., McGowan, J. J. and Smith, C. W., "Experimental Determination of Side Boundary Effects on Stress Intensity Factors in Surface Flaws", VPI-E-74-5, 21 pages, March 1974 (In Press) J. of Engineering Materials and Technology.
- [24] Schroedl, M. A. and Smith, C. W., "A Study of Near and Far Field Effects in Photoelastic Stress Intensity Determination", VPI-E-74-13, 40 pages, July 1974.
- [25] McGowan, J. J. and Smith, C. W., "A Finite Deformation Analysis of the Near Field Surrounding the Tip of Small, Crack-Like Ellipses", VPI-E-74-10, 79 pages, May 1974.

- [26] Dixon, J. R. and Strannigan, J. S., "A Photoelastic Investigation of the Stress Distribution in Uniaxially Loaded Thick Plates Containing Slits", NEL Report No. 288, National Engineering Laboratory, Glasgow, Scotland, May 1967.
- [27] Gross, B. E. and Mendelson, A., "Plane Elasto-static Analysis of V-Notched Plates", International Journal of Fracture Mechanics 8, 3, 267-376, September 1972.
- [28] Brown, W. F., Jr. and Srawley, J. E., "Fracture Toughness Testing", Fracture Toughness Testing and Its Applications, ASTM STP 381, 133-196, 1964.
- [29] Brown, W. F., Jr., Plane Strain Crack Toughness Testing of High Strength Metallic Materials ASTM STP 410, December 1967.
- [30] Irwin, G. R., "Measurement Challenges in Fracture Mechanics", William Murray Lecture SESA Fall Meeting, Indianapolis, Ind., October 1973.
- [31] Rice, J. R., "A Path Independent Integral and the Approximate Analysis of Strain Concentration by Notches and Cracks", J. of Applied Mechanics, 379-386, June 1968.
- [32] Paris, P. C. and Sih, G. C., "Stress Analysis of Cracks", Fracture Toughness Testing and Its Applications, ASTM STP-381, 30-81, 1965.
- [33] Collipriest, J.E., Jr. and Thatcher, C. S., "Cyclic Crack Growth in Aluminum Alloy 2024-T851", SD73-SH-0070, Space Division, Rockwell International, Downey, Calif., August 1973.
- [34] Gross, B. and Srawley, J. E., "Stress Intensity Factors for Single Edge Notch Specimens in Bending or Combined Bending and Tension by Boundary Collocation of a Stress Function", NASA TN D-2603, January 1965.
- [35] Smith, F. W., "Stress Intensity Factors for a Surface Flawed Fracture Specimen", TR-1, Dept. of Mechanical Engineering, Colorado State University, September 1971.



TABLE 1  
Test Results for Edge Cracks

Type of Notch	Stress Freezing Tests							Room Temperature Tests	
	R-H	R-L	V-H	V-L	N-H	N-L	V	N	
Number of Replications	5	1	5	2	2	1	2	1	
Remote Stress kPa	70.3	42.2	76.4	43.04	34.6	21.1	3053	2352	
$\left[ \frac{K_{TSCM}}{K_{Th} a} \right]_{avg}$	1.25	1.18	1.12	1.14	1.08	1.13	1.02	1.03	
$\left[ \frac{K_{TSCM}}{K_{Th} a} \right]_{Range}$	1.23 to 1.29		1.08 to 1.15	1.11 to 1.17	1.04 to 1.12		1.00 to 1.04		
$\left[ \frac{K_{TSCM}}{K_{Th} a} \right] \frac{(1-\nu^2)^{1/2}}{0.955^+}$	1.13	1.07	1.02	1.03	0.97	1.02	0.99	1.00	

a - Theoretical SIF Gross-Srawley Solution  
Average Material fringe value 254 N/m/order

R-H Rectangular-High Load  
R-L Rectangular-Low Load  
V-H Vee-High Load  
V-L Vee-Low Load  
N-H Natural-High Load  
N-L Natural-Low Load

$$+0.955 = \{1 - [0.3]^2\}^{1/2}$$

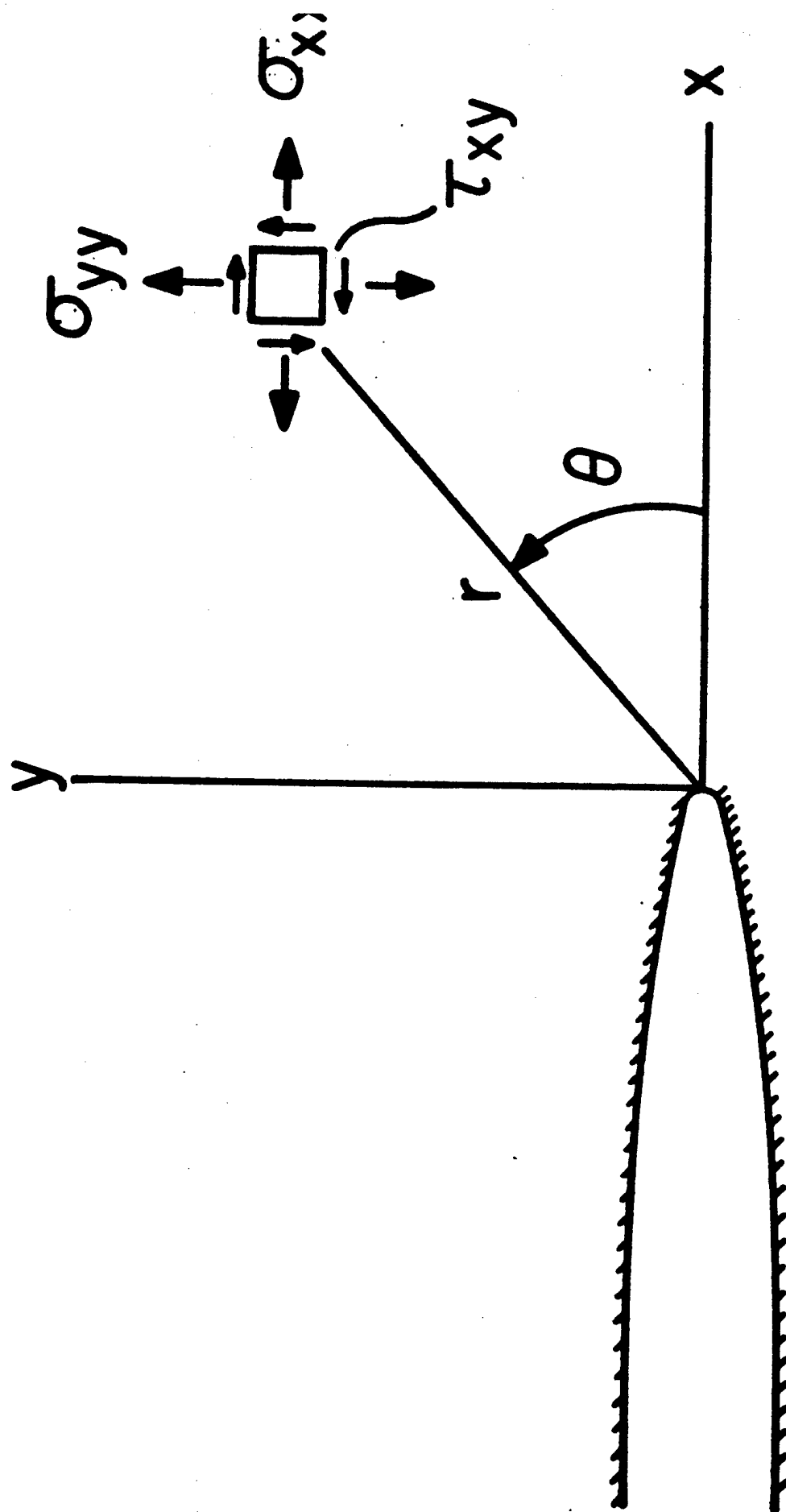


Figure 1. Notation

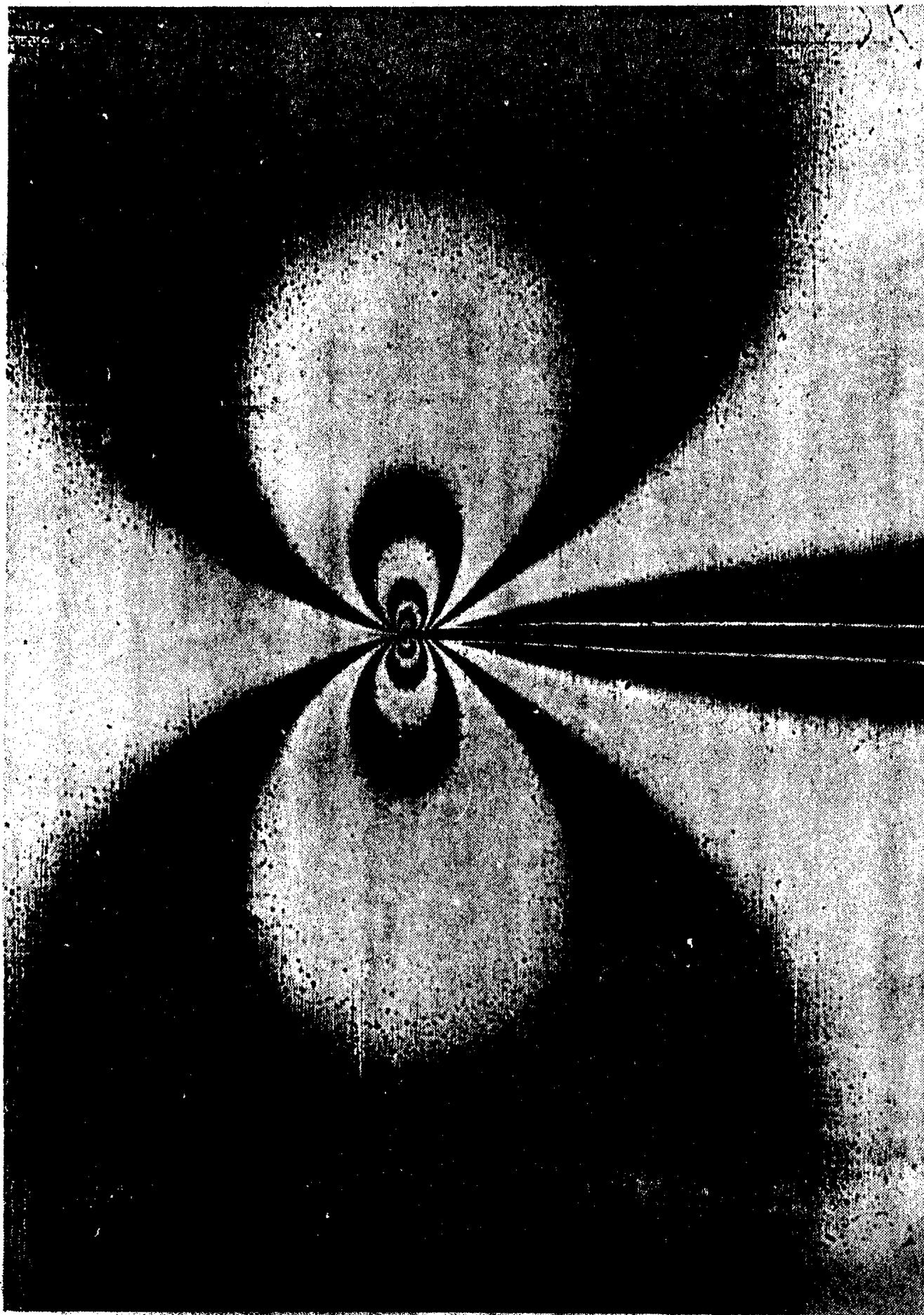


Figure 2. Spreading of Fringes Normal to Crack Plane (Mode I)

27

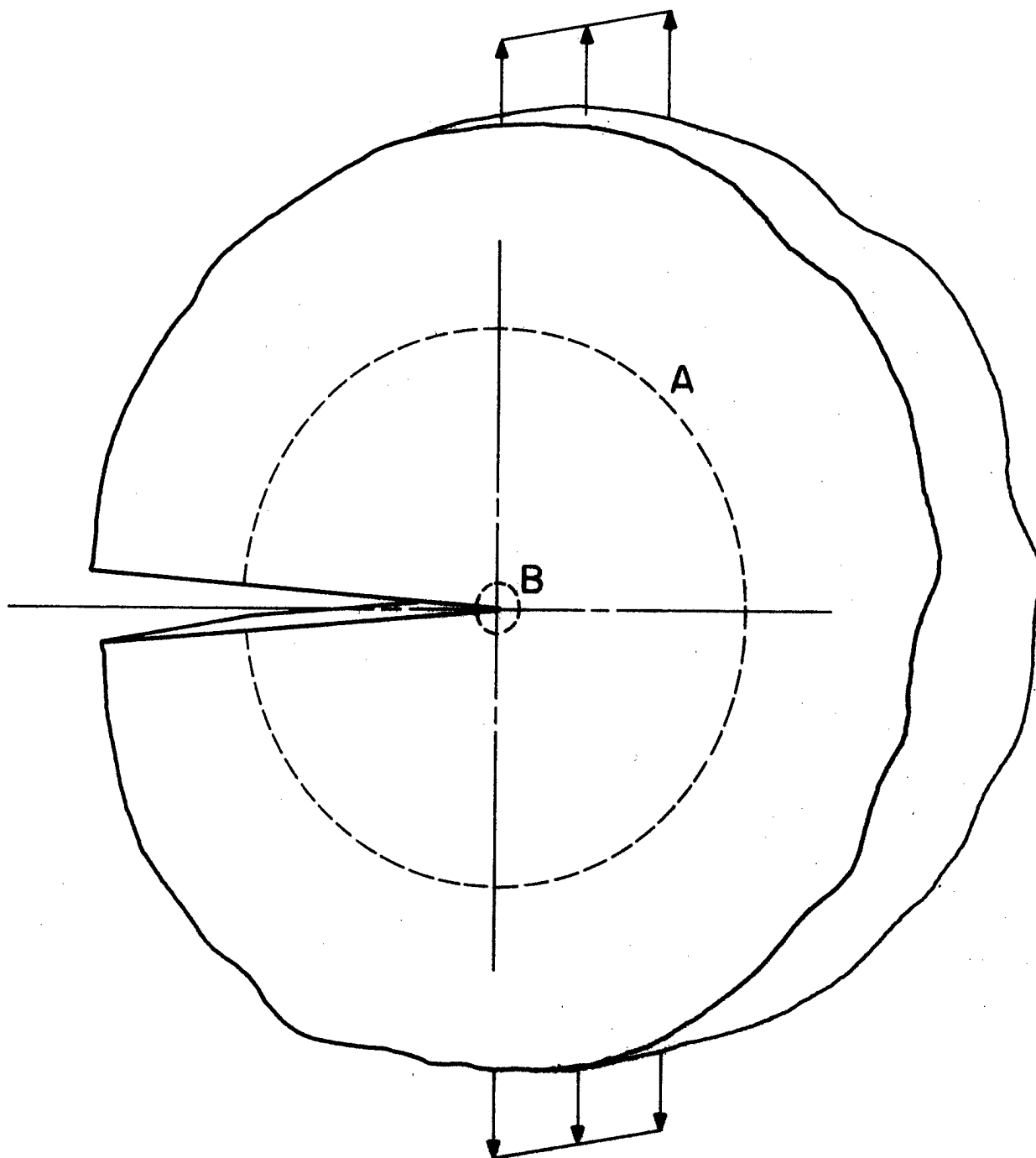
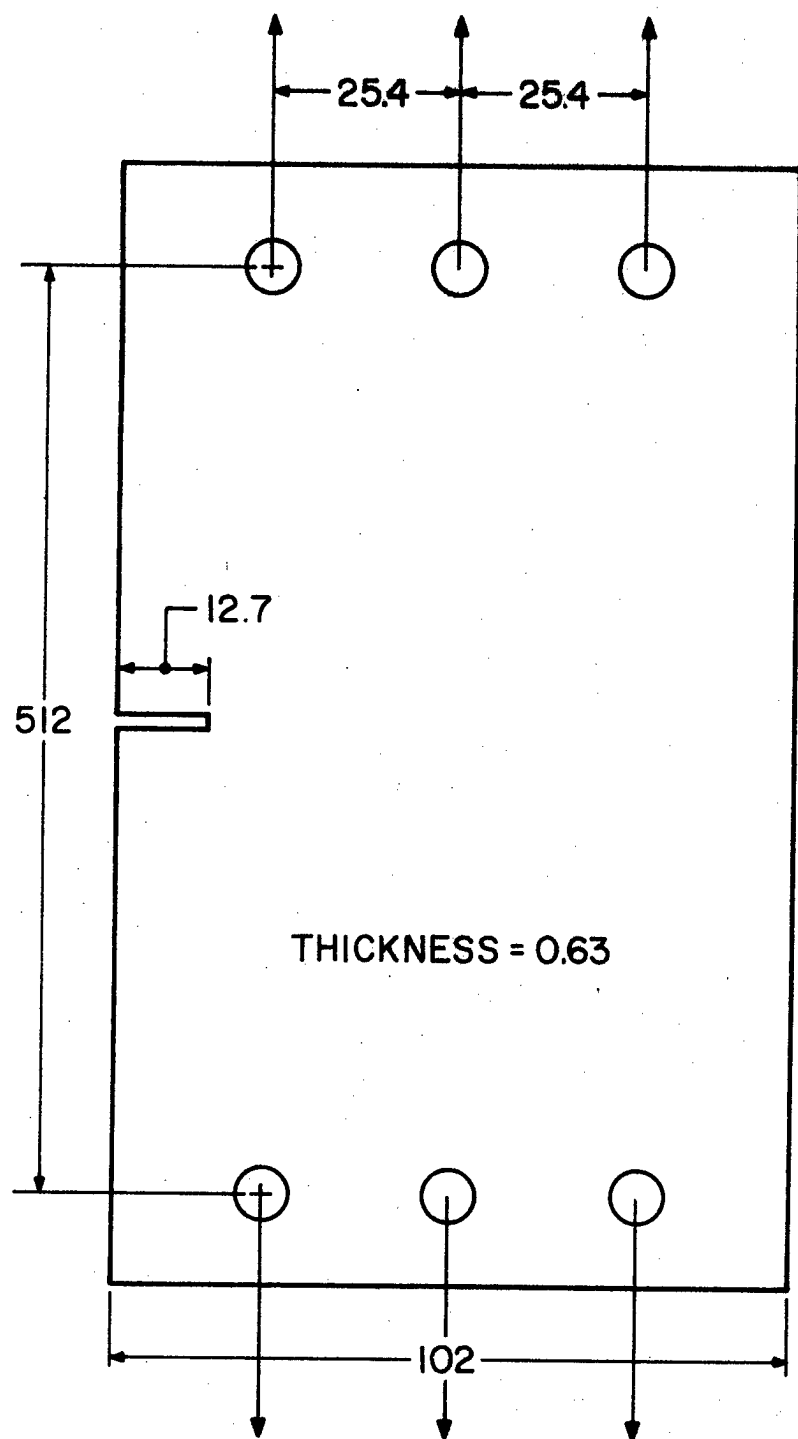
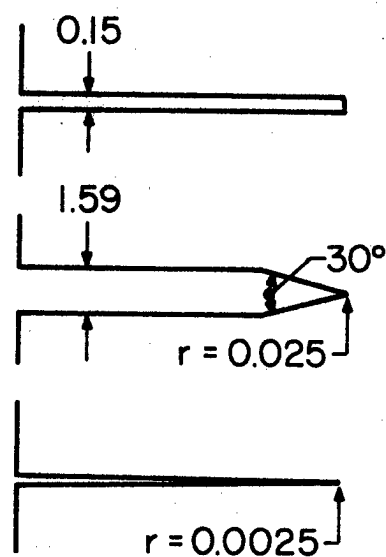


Figure 3. Generalized Plate Specimen



### CRACK GEOMETRIES



ALL DIMENSIONS  
IN MILLIMETERS

PLATE DIMENSIONS ARE  
NOMINAL DIMENSIONS

Figure 4. Specimen Geometry and Loading.

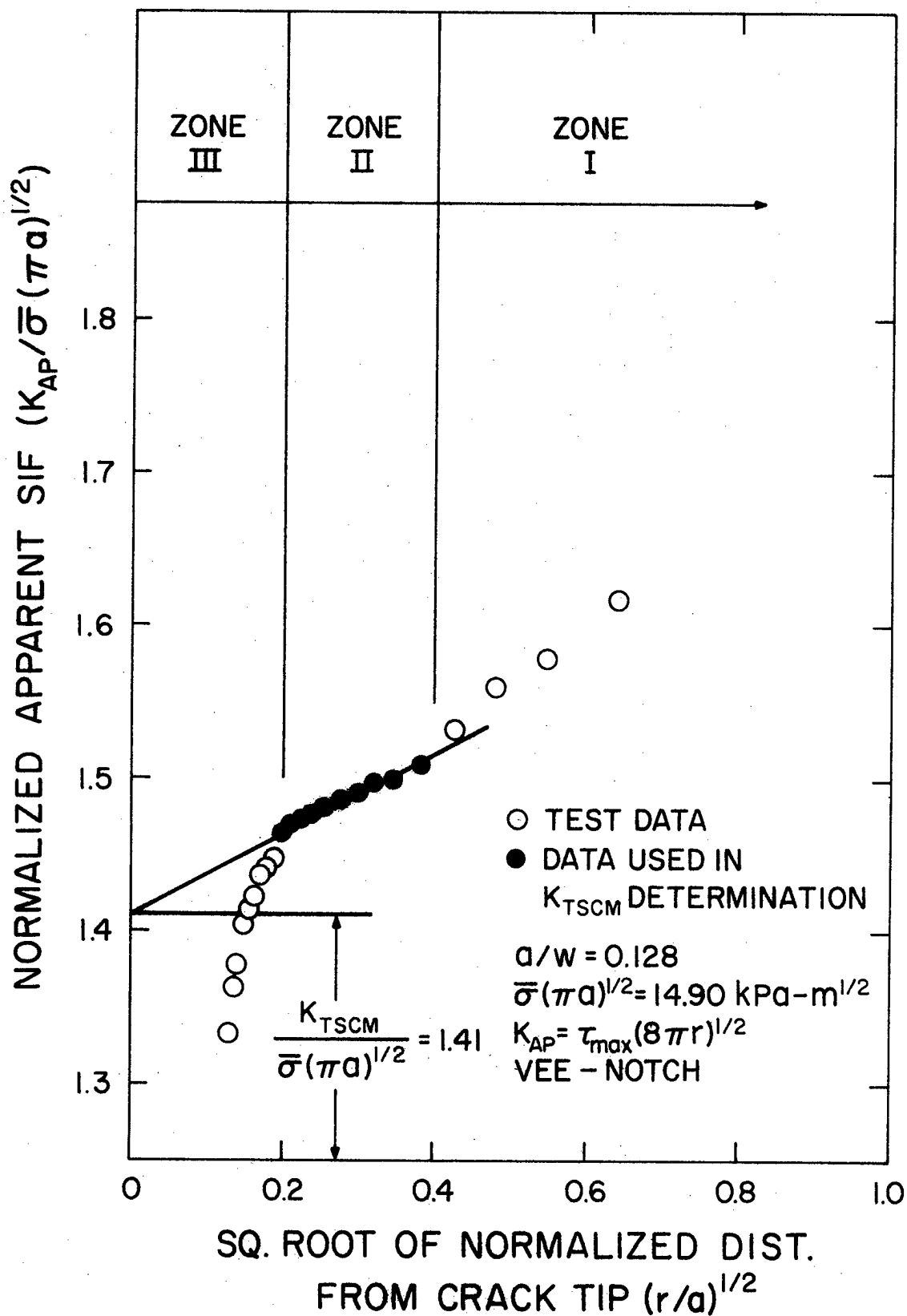


Figure 5. Normalized  $K_{AP}$  vs  $r^{1/2}$  A Typical Result

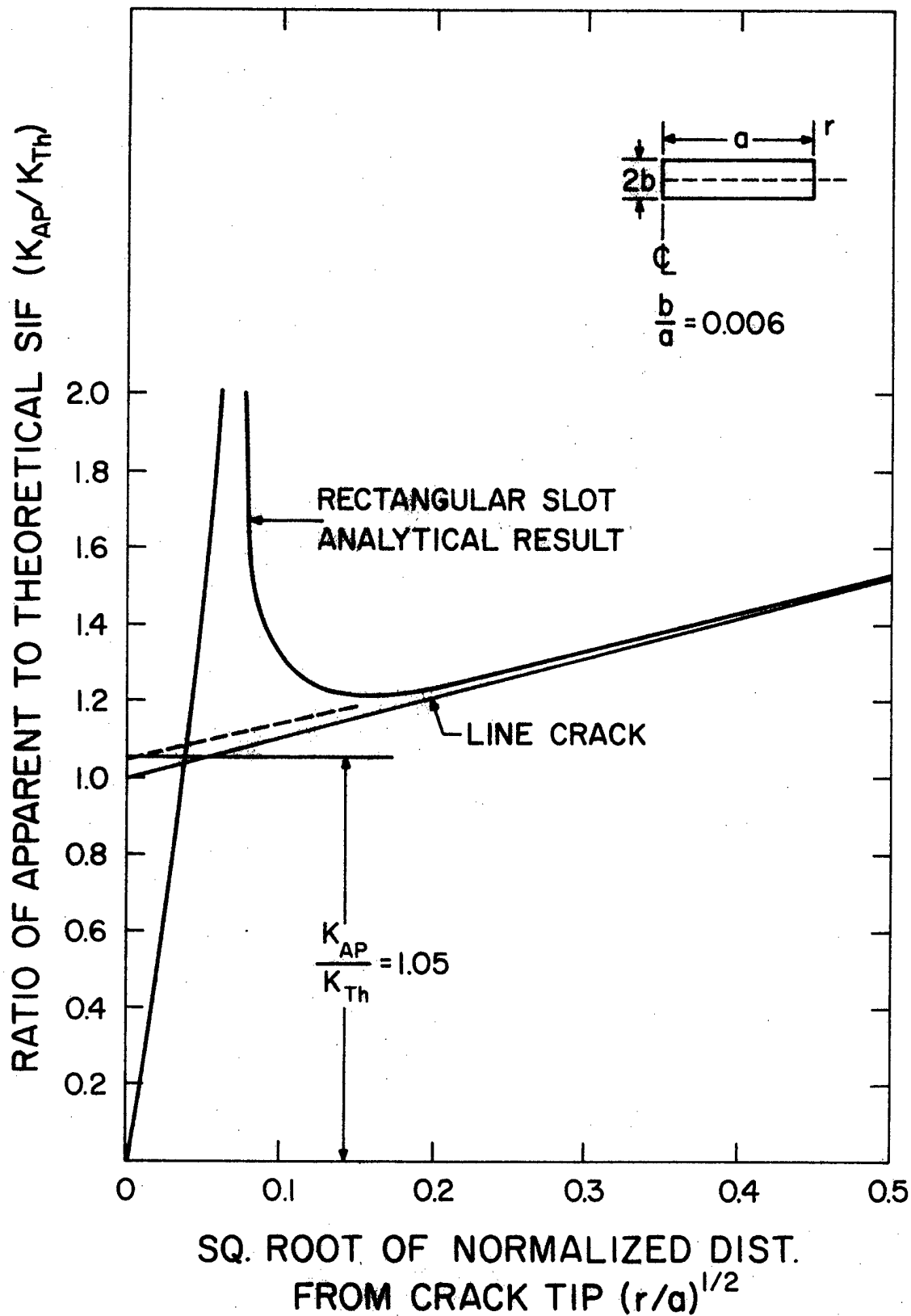


Figure 6. Normalized  $K_{Ap}$  vs  $r^{1/2}$  Rectangular Slot

## DISTRIBUTION LIST

(Virginia Polytechnic Institute  
and State University)

Commanding General  
U.S. Army Natick Laboratories  
ATTN: Mr. E. W. Ross, Jr.  
Natick, Mass. 01762

Lehigh University  
ATTN: Dr. G. C. Sih  
Bethlehem, Pa. 18015

Commanding Officer  
Frankford Arsenal  
ATTN: Mr. P. D. Flynn  
Bridge & Tacony Streets  
Philadelphia, Pa. 19137

Battelle Memorial Institute  
ATTN: Dr. G. T. Hahn  
505 King Avenue  
Columbus, Ohio 43201

General Electric Company  
ATTN: A. J. Brothers, Materials and  
Processes Lab.  
Schenectady, New York 12010

United States Steel Corporation  
ATTN: Mr. S. T. Rolfe, Applied  
Research Lab.  
Monroeville, Pa. 15146

University of Illinois  
ATTN: Mr. H. T. Corten, Department of  
Theoretical & Applied Mechanics  
212 Talbot Lab.  
Urbana, Illinois 61803

Westinghouse Electric Company  
ATTN: Mr. E. T. Wessel, R&D Center  
Pittsburgh, Pa. 15200

Carnegie Institute of Technology  
ATTN: Dr. J. L. Swedlow  
Schenley Park  
Pittsburgh, Pa. 15213

Rensselaer Polytechnic Institute  
ATTN: Prof. J. C. Janz, Chairman of  
Chemistry Department  
Troy, New York 12180

Syracuse University  
ATTN: Dr. H. W. Liu  
Syracuse, New York 13210

Commanding Officer  
U.S. Army Aviation Material  
Laboratories  
ATTN: Mr. C. D. Roach  
Fort Eustis, Virginia 23604

University of California  
ATTN: W. W. Gerberich, Department of  
Mineral Technology  
Berkeley, Calif. 94700

University of Illinois  
ATTN: Prof. D. Drucker, Deah of School  
of Engineering  
Champaign, Illinois 61820

University of Washington  
ATTN: Prof. A. Kobayashi, Department  
of Mechanical Engineering  
Seattle, Washington 98105

Technical Director  
U.S. Army Materials & Mechanics  
Research Center  
ATTN: Mr. J. Bluhm  
Watertown, Mass. 02172

Brown University  
ATTN: Dr. J. R. Rice  
Providence, Rhode Island 02912

University of Connecticut  
ATTN: Dr. A. J. McEvily, Head,  
Dept. of Metallurgy U-139  
Dr. N. D. Greene, Metallurgy  
Dept.  
Storrs, Conn. 06268



Copies

Director Naval Research Laboratory Attn: Dr. J. M. Krafft, Code 8430 Mr. W. S. Pellini, Code 6300 Washington, D.C. 20390	1 1
Dr. G. R. Irwin University of Maryland Department of Mechanical Engineering College Park, Maryland 20742	1
Commander Wright-Patterson Air Force Base ATTN: AFML(MAAA) Hq., Aeronautical Systems Division Ohio 45433	5
Commander George C. Marshall Space Flight Center ATTN: M-S&M-M M-F&AEM, Bldg. 4720 Huntsville, Alabama 35809	1 1
NASA Scientific and Technical Information Facility ATTN: Acquisitions Branch P. O. Box 33 College Park, Maryland 20740	1
Mr. Robert L. Shannon, Extension Manager U.S. Atomic Energy Commission Division of Technical Information Ext. P. O. Box 62 Oak Ridge, Tennessee 37831	2
Defense Metals Information Center Battelle Institute 505 King Avenue Columbus, Ohio 43201	1
Commanding Officer U.S. Army Materials Research Agency ATTN: AMXMR-Technical Information Center Watertown, Mass. 02172	2
Commanding General Aberdeen Proving Ground ATTN: AMXCC - Dr. C. Pickett AMXCC - Technical Library Maryland 21003	1 1
Commanding Officer U.S. Army Mob Equip Research & Dev. Center ATTN: Technical Documents Center Fort Belvoir, Va. 22060	2
Commanding General U.S. Army Electronics Command Fort Monmouth, New Jersey 07703	1

Copies

Commandant HQ, U.S. Army Aviation School ATTN: Office of the Librarian Fort Rucker, Alabama 36362	1
Commanding Officer Frankford Arsenal Philadelphia, Pa. 19137	1
Commanding Officer Picatinny Arsenal Dover, New Jersey 07801	1
Commanding General Redstone Arsenal ATTN: Documentation & Technical Information Branch AMSMI-RRS AMSMI-RKK AMSMI-RSM Alabama 35809	2 1 1 1
Commanding Officer Plastics Technical Evaluation Center ATTN: SMUPA-VP3 Picatinny Arsenal Dover, New Jersey 07801	1
Commanding Officer Watervliet Arsenal ATTN:  SWEWV-RDR Dr. M. Hussain  SWEWV-RDR Dr. J. H. Underwood SWEWV-RDR Mr. J. F. Throop	  1  1 1
Watervliet, New York 12189	
Mr. George Vrooman SWEWV-RDT-6 Document Libraries Watervliet Arsenal Watervliet, New York 12189	1
Mr. Charles Eldridge Structures and Mechanics Laboratory Research and Development Director U. S. Army Missile Command Huntsville, Alabama	1
Commanding Officer Watervliet Arsenal ATTN: SWEWV-RDT-TP, Mr. John Barnewall Watervliet, New York 12189	6

No. of  
Copies

Office of the Director of Defense Research & Engineering  
ATTN: Assistant Director of Materials  
The Pentagon  
Washington, D. C. 20315

1

Commander  
Defense Documentation Center  
Cameron Station, Bldg. 5  
5010 Duke Street  
Alexandria, Virginia 22314

12

Commanding General  
U.S. Army Material Command  
ATTN: AMCRD  
AMCRD-R, Mr. H. Cohen  
AMCRD-W  
AMCRD-TC

1

1

1

1

Bldg. T-7  
Washington, D. C. 20315

Commanding General  
U.S. Army Weapons Command  
ATTN: AMSWE-LCD  
AMSWE-PPR  
AMSWE-RDA  
AMSWE-RDR

1

1

1

1

Rock Island, Illinois 61201

Commanding General  
U.S. Army Tank-Automotive Command  
ATTN: AMSTA-BSL  
AMSTA-BMM  
Warren, Michigan 48090

1

1

Commanding General  
U.S. Army Munitions Command  
ATTN: AMSMU-SS-EC  
Dover, New Jersey 07801

1

Commanding Officer  
Army Research Office  
Office Chief Research & Development  
ATTN: Physical Sciences Division  
3045 Columbia Pike  
Arlington, Virginia 22207

2

Commanding Officer  
U.S. Army Research Office (Durham)  
Box CM, Duke Station  
Durham, North Carolina

6

Commanding Officer  
Rock Island Arsenal  
ATTN: SWERI-RDD  
Rock Island, Illinois 61202

1

DISTRIBUTION LIST - 1 Copy Each

Mr. J. G. Kaufman  
Alcoa Research Laboratory  
P. O. Box 772 Freeport Rd.  
New Kensington, Pa. 15068

Dr. T. D. Dudderar  
Room 1A-105  
Bell Telephone Labs  
Mountain Avenue  
Murray Hill, N. J. 07971

Mr. W. F. Brown  
NASA  
Lewis Research Center  
Cleveland, Ohio 44135

Dr. Royce Forman  
NASA  
Manned Spacecraft Center  
Houston, Texas 77058

Dr. F. W. Smith  
Dept. of Mechanical Engineering  
Colorado State University  
Fort Collins, Colorado 80521

Mr. N. G. Tupper  
AFFDL/FBA  
Wright-Patterson AFB, Ohio 45433

NASA Langley Research Center  
Hampton, Va. 23365  
ATTN: Dr. J. R. Davidson

Mr. Howard Wood  
AFFDL/FBA  
Wright-Patterson AFB, Ohio 45433

Mr. Al Gunderson  
AFFDL/FBA  
Wright-Patterson AFB, Ohio 45433

Dr. Ramesh Shah  
The Boeing Aerospace Co.  
Mail Stop 8C-45  
P. O. Box 3999  
Seattle, Washington 98124

Dr. J. E. Srawley  
NASA  
Lewis Research Center  
Cleveland, Ohio 44135

Dr. E. E. Saibel  
U.S. Army Research Office  
Box CM Duke Station  
Durham, N. C. 27706

Dr. N. Basdekis  
Structural Mechanics Branch  
Mathematics and Information Sciences Division  
Office of Naval Research  
800 N. Quincy Blvd.  
Arlington, Va. 22217

Mr. Thomas W. Orange  
NASA Lewis Research Center  
21000 Brook Park Road, 49-3  
Cleveland, Ohio 44135

Dr. B. R. Mullinix  
Dept. of the Army  
USA-MICOM  
AMSMI-RLA  
Building 5400  
Redstone Arsenal, Ala. 35809

Dr. J. C. Newman, Jr.  
Materials Division  
Structural Integrity Branch  
Mail Stop 465  
Langley Research Center  
Hampton, Va. 23365

Mr. William Walker  
U.S. Air Force Office of  
Scientific Research  
1400 Wilson Blvd.  
Arlington, Va. 22217